

Evaluation of Nozzle Coefficients for Water Jet Used in Sewer Cleaning

PhD. Eng. Nicolae MEDAN

¹Tech. Univ. Cluj-Napoca, North Univ. Center Baia Mare, Nicolae.Medan@cunbm.utcluj.ro

Abstract: The purpose of this paper is to determine the discharge, speed and contraction coefficients for nozzle with three dimensions of diameter. To determine the speed of water jet at the nozzle exit, were measured the impact forces between the water jet and a flat and rigid surface in the potential core region of the water jets. In order to measure the impact forces of water jet, were designed and built a stand for generating pressure jets, as well as a device to measure the impact force.

Keywords: water jet, impact force, discharge coefficient, speed coefficient, contraction coefficient.

1. Introduction

Industrial cleaning is a classic application of water jets technology. In the late 1950s, when reliable high pressure pumps were built, the usage of water jets spread widely in the field of pipes and sewerage cleaning. Phenomena that occur in the cleaning water jets are complex. Adler [1] describes mechanisms occurring at the impact of a jet with a surface. Leach et al [6], Leu et al [7] and Guha et al [5] analysed pressure distribution along centreline of the water jet. A number of papers have studied the influence of nozzle geometry on water jet [2, 3, 4, 8].

In order to be able to characterize the degree of efficiency of the nozzles has been defined the discharge coefficient μ . This coefficient is determined by the speed coefficient ϕ , the contraction coefficient ε and the compressibility coefficient ψ of the water from the jet.

To determine the coefficients for the nozzles used in this paper, were made a series of measurements for the determination of the impact force of the water jets.

2. Apparatus used and methodology of the measurements

In order to measure the impact forces of water jet, were designed and built a stand for generating pressure jets, as well as a device to measure the impact force [9].

2.1 Stand to generate pressure jet

Schematic diagram of the stand to generate pressure jet is shown in figure 1.

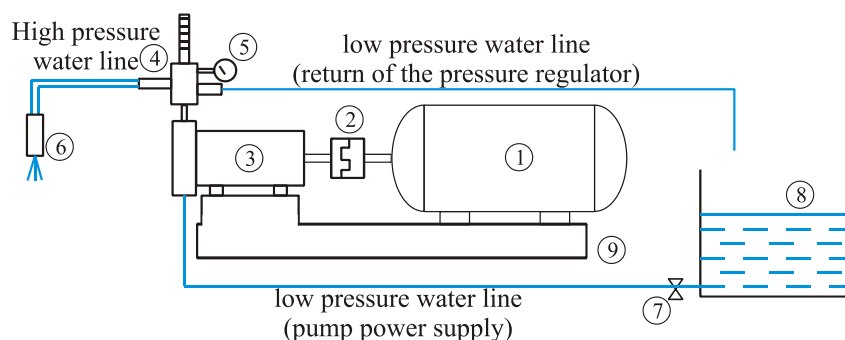


Fig. 1. Schematic diagram of the stand to generate pressure jet [9]

Component parts of stand: (1) electric motor (2) flexible coupling; (3) high pressure pump, 4) pressure regulator, 5) pressure gauge, 6) nozzle, 7) tap water, 8) water tank, 9) chassis.

Water coming out of the high pressure pump (3) goes into the pressure regulator (4). Through it adjusts the pressure and flow of water in the path of the high pressure water. This pressure corresponds to the one at the outlet of nozzle.

2.2 Device for the measurement of the impact force

In figure 2 is represented the principle diagram of the device for the measurement of the impact force of the water jet and a flat and rigid surface.

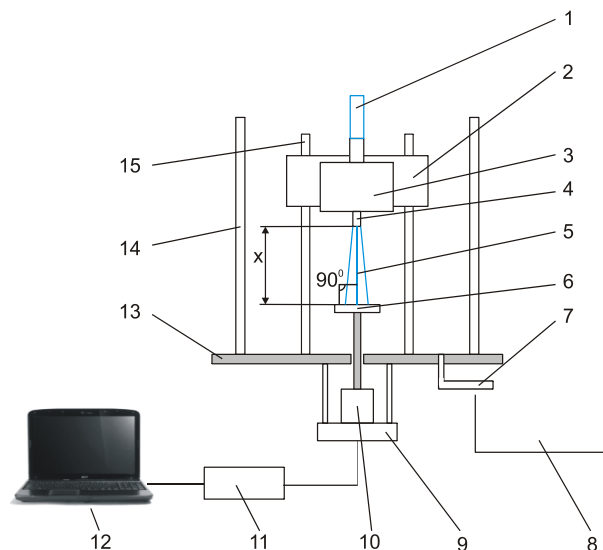


Fig. 2. Diagram of the device for the measurement of the impact force of the water jet [9]

Main component parts of the device are: 1) high-pressure water hose, 2) support nozzle, 3) nozzle block, 4) nozzle, 5) water jet, 6) flat and rigid target plate, 7) collection path water, 8) scaled container for measurement of the flow of water jet, 9) piezoelectric sensor mounting, 10) piezoelectric sensor, 11) data acquisition Personal Daq/3000, 12) computer for the processing of data; 13) support plate, 14) acrylic tube, 15) rods for adjusting distance x .

From high pressure water hose (1) come water at a certain pressure p desired. At the outlet of nozzle is generated a water jet (5) that striking target plate (6), who is located at a certain distance x in front of the nozzle. The jet (5) generates an impact force at a time when he meets target plate (6). This force produces axial movement of target plate. This movement is converted into an electric signal by the piezoelectric sensor (10). Electrical signal is collected by data acquisition Personal Daq/3000 (11), which forward data to a computer (12) using DaqView soft processes data actually obtained.

2.3 Geometric configuration of nozzles

Geometric configuration of the nozzles used is shown in figure 3.

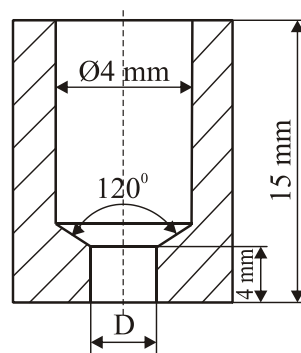


Fig. 3. Geometric configuration of the nozzles

The values used for diameter D of nozzle are $D=1\text{ mm}$, 1.5 mm and 2 mm . The material for nozzles is stainless steel.

3. Results

The structure of the high speed water jets in air can be divided into three distinct regions [7,10]: 1) potential core region, 2) main region and 3) diffused droplet region.

It is known that in the potential core region, which has been determined as having a length of 6 to 8 times the diameter of the nozzle diameter [5], the water speed is relatively constant and equal to the speed of the water jet at the outlet of the nozzle. Thus, in order to be able to calculate the speed coefficient φ , we calculated the impact forces generated by the water jet at a distance of 8 mm for all three dimensions D of the nozzles, distance which corresponds to the potential core region of the water jet.

The Bernoulli equation of equilibrium, in the form of pressure for a water jet of under pressure is:

$$p_1 + \rho \cdot g \cdot h_1 + \frac{1}{2} \rho v_1^2 = p_2 + \rho \cdot g \cdot h_2 + \frac{1}{2} \rho v_2^2 + p_v \quad (1)$$

Starting on Bernoulli equation (1) can be expressed the velocity of the water speed V at the outlet of the nozzle, depending on pressure p of the water (upstream of the nozzle):

$$V = \sqrt{2 \frac{(p - p_v)}{\rho}} = \sqrt{2 \frac{p \left(1 - \frac{p_v}{p}\right)}{\rho}} \text{ [m/s]} \quad (2)$$

where:

- p is the regulated pressure upstream of the nozzle;
- p_v is the loss pressure in the nozzle;
- ρ is the density of the water.

Is defined speed coefficient φ given by the relationship:

$$\varphi = \sqrt{1 - \frac{p_v}{p}} \quad (3)$$

Replacing the relationship (3) in the relationship (2) the equation for the speed V becomes:

$$V = \varphi \sqrt{\frac{2p}{\rho}} \text{ [m/s]} \quad (4)$$

Considering the pressure loss in the nozzle $p_v=0$, resulting $\varphi=1$ and under these conditions, from the relationship (4), it is possible to calculate the theoretical speed V_{th} of the water at the outlet of the nozzle with relationship:

$$V_{th} = \sqrt{\frac{2p}{\rho}} \text{ [m/s]} \quad (5)$$

In accordance with the theoretical speed V_{th} of the water at the outlet of the nozzle may be calculated theoretical flow rate Q_{th} of the water at the outlet of the nozzle with relationship:

$$Q_{th} = \pi \left(\frac{D^2}{4} \right) V_{th} \text{ [m}^3\text{/s]} \quad (6)$$

where D is the diameter of the nozzles.

The pressures p used to perform the measurements have the values $p=100$ bar, $p=120$ bar, $p=140$ bar, $p=160$ bar, $p=180$ bar and $p=200$ bar.

They have measured the real flow rates Q_{mas} of water. Has been measured the flow rate of water for a period of 60 seconds for each diameter D of the nozzle and for the six established pressures. For the measurement of flow rate has been used a graduated container. For the accuracy of the

flow rate measurement for each set of parameters have been carried out a number of three measurements, and still has been used in the arithmetic average.

In table 1 are presented the theoretical flow rates Q_{th} with relationship (6) and the measured flow rates Q_{mas} (using the stand to generate pressure jet (fig.1) and the device for the measurement of the impact force (fig. 2).

TABLE 1: Theoretical and measured flow rates

Pressure [bar]		100	120	140	160	180	200
Nozzle [mm]							
1	Q_{th} [m ³ /s]	0.000107	0.000118	0.000128	0.000136	0.000145	0.000153
	Q_{mas} [m ³ /s]	0.00008	0.00008	0.00009	0.00010	0.00010	0.00011
1,5	Q_{th} [m ³ /s]	0.000242	0.000265	0.000287	0.000307	0.000326	0.000343
	Q_{mas} [m ³ /s]	0.00017	0.00019	0.00020	0.00022	0.00024	0.00025
2	Q_{th} [m ³ /s]	0.000431	0.000472	0.00051	0.000546	0.000579	0.00061
	Q_{mas} [m ³ /s]	0.00031	0.00035	0.00038	0.00041	0.00044	0.00046

According to the values presented in table 1, it should be noted that there is a difference between the theoretical flow rates Q_{th} and measured flow rates Q_{mas} . This difference is due to the discharge coefficient μ . Practically this coefficient provides information on the effectiveness of the nozzle. The discharge coefficient μ shall be expressed using the relationship [2]:

$$\mu = \frac{Q_{mas}}{Q_{th}} \tag{7}$$

Using the relationship (7) and the values obtained at the table 1, it was determined the values of discharge coefficient μ , values presented in table 2.

TABLE 2: The discharge coefficient μ

Nozzle [mm]	p [bar]					
	100	120	140	160	180	200
	μ					
1	0.687	0.689	0.693	0.689	0.698	0.694
1,5	0.676	0.692	0.687	0.707	0.718	0.715
2	0.707	0.716	0.715	0.730	0.732	0.727

Based on the values of discharge coefficient μ obtained in table 2, it was realised the graph presented in figure 4.

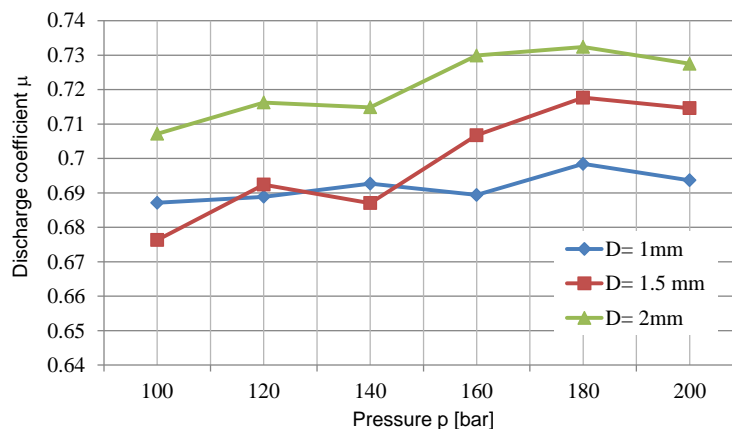


Fig. 4. Discharge coefficient μ

Conclusion: The discharge coefficient μ increases with pressure increasing. For the nozzle with diameter $D = 2\text{mm}$ we are dealing with a higher efficiency than for the other two diameters of the nozzle. For all three dimensions of the nozzle the maximum value of the discharge coefficient μ appears for the pressure of 180 bar.

The discharge coefficient μ is given by the relationship (Anoni et al 4):

$$\mu = \varphi \cdot \varepsilon \cdot \psi \quad (8)$$

where:

- φ is the speed coefficient;
- ε is the contraction coefficient;
- ψ is the compressibility of the water.

In this paper, the volume of flow variation has values between $3.438 \times 10^{-7} \text{ [m}^3/\text{s]}$ for $p=100$ bar and $4.11 \times 10^{-6} \text{ [m}^3/\text{s]}$ for $p=200$ bar. Therefore the coefficient of compressibility ψ can be neglected ($\psi=1$).

The speed coefficient φ is given by relationship [2]:

$$\varphi = \frac{V_r}{V_{th}} \quad (9)$$

where:

- V_r is the real speed of water jet at the outlet of the nozzle;
- V_{th} is the theoretical speed of water jet at the outlet of the nozzle.

The impact force of a water jet is given by the relationship [2]:

$$F = \rho \cdot Q_{mas} \cdot V_r \text{ [N]} \quad (10)$$

From relationships (9) and (10) result:

$$\varphi = \frac{F \sqrt{\rho}}{\rho \cdot Q_{mas} \sqrt{2p}} \quad (11)$$

In table 3 are presented the values of impact forces measured for a standoff distance $x=8$ mm.

TABLE 3: The measured impact forces for $x=8$ mm

Nozzle [mm]	p [bar]					
	100	120	140	160	180	200
	F [N]					
1	10.78	12.40	14.59	16.46	18.89	21.47
1,5	23.14	28.11	31.83	37.39	43.32	48.09
2	39.84	48.55	57.78	64.22	74.57	85.67

Using the relationship (11) and the values of measured impact forces from table 3 shall be calculated the speed coefficient φ . In table 4 are presented the determined values of speed coefficient φ .

TABLE 4: The speed coefficient φ

Nozzle [mm]	p [bar]					
	100	120	140	160	180	200
	φ					
1	0.999	0.955	0.958	0.950	0.957	0.985
1.5	0.968	0.957	0.936	0.936	0.949	0.952
2	0.897	0.899	0.919	0.875	0.900	0.937

Based on the values of speed coefficient φ obtained in table 4, it was realised the graph presented in figure 5.

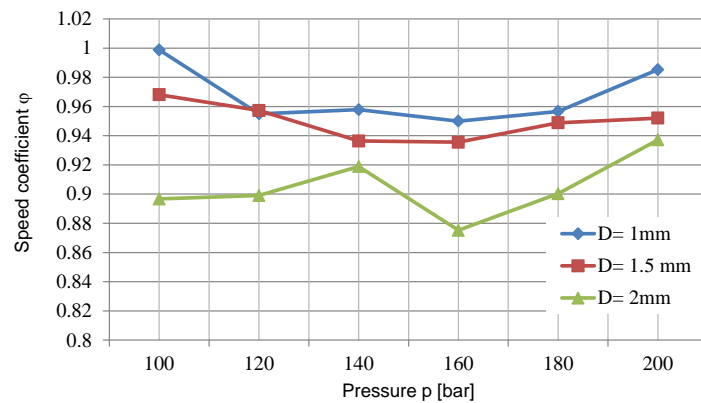


Fig. 5. Speed coefficient φ

Conclusion. The speed coefficient φ decreases with increasing of the diameter of the nozzle. For values of diameters $D=1$ mm and $D=1.5$ mm the speed coefficient φ is maximum for pressure $p=100$ bar and for Diameter $D=2$ mm is maximum for $p=200$ bar.

After they have been calculated the discharge coefficients μ and speed coefficients of φ , using the relationship (8) may be calculate the contraction coefficient ε for all three dimensions of the nozzle:

$$\varepsilon = \frac{\mu}{\varphi} \tag{12}$$

The calculated values for the contraction coefficient ε are presented in the table 5.

TABLE 5: The contraction coefficient ε

Nozzle [mm]	p [bar]					
	100	120	140	160	180	200
	ε					
1	0.688	0.721	0.723	0.726	0.730	0.704
1.5	0.699	0.723	0.734	0.755	0.756	0.751
2	0.789	0.797	0.778	0.834	0.814	0.776

Based on the values of contraction coefficient ε obtained in table 5, it was realised the graph presented in figure 6.

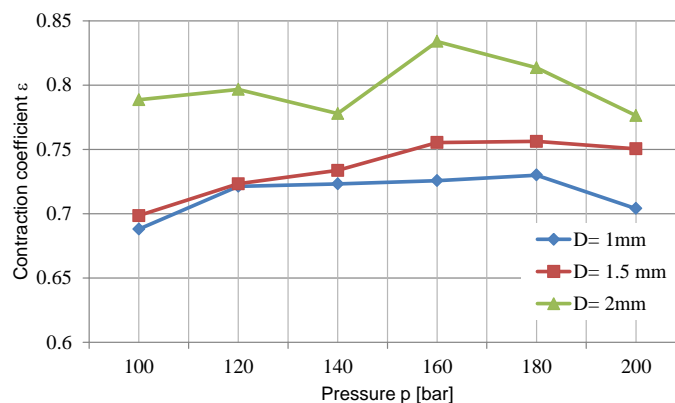


Fig. 6. Contraction coefficient ε

Conclusion: From the graph 5 it is observed that for the nozzles $D=1$ mm and $D=1.5$ mm minimum value of the contraction coefficient appears for $p=100$ bar and the maximum value appears for $p=180$ bar, while for the nozzle with $D=2$ mm minimum value of the contraction coefficient appears for $p=140$ bar and the maximum value appears for $p=160$ bar.

4. Conclusions

In this work it is presented a methodology for the determination the efficiency of the nozzles used to sewer cleaning. In order to be able to determine the effectiveness of the nozzles were determined: discharge coefficient μ , speed coefficient φ and contraction coefficient ε .

By determining the theoretical and practical of mass flow of the water jets has been determined the discharge coefficient μ , coefficient which practically represents the efficiency of the studied nozzles.

In the experimental domain of this work, the compressibility coefficient ψ of the water in the jet shall have the value of 1. Therefore the coefficient of compressibility ψ can be neglected.

In order to determine the speed coefficient φ were carried out the measurements of the impact forces in potential core region of the water jet (where the water speed is relatively constant and equal to the speed of the water jet at the outlet of the nozzle).

After the determination of the discharge coefficient μ and the speed coefficient φ could be determined the contraction coefficient ε .

The efficiency of the nozzles concerned depends by the diameter of the nozzles and the pressure of a water jet at the outlet of the nozzle.

For all three dimensions of the nozzles maximum efficiency appears for pressure $p=180$ bar.

References

- [1] W. F. Adler, "The Mechanics of Liquid Impact", Treatise on Materials Science and Technology, 1979. pp. 127-183;
- [2] M. Annoni, L. Cristaldi, M. Faifer, M. Norgia, "Orifice Coefficients Evaluation for Water Jet Application", Sept. 22-24, 2008, Florence, Italy, 16th IMECO TC4 Symposium, "Exploring New Frontiers of Instrumentation and Method for Electrical and Electronic Measurement", pp. 761-766;
- [3] A., Cotetiu, R., Cotetiu, N. Ungureanu, "Research about automatic adjustment solution of the advance force at the perfusion drills using fluid elements", January 2014, "Archives of Mining Sciences", Volume 58, Issue 4, ISSN (Print) 0860-7001, pp. 1201-1208;
- [4] S. Dimitrov, S. Simeonov, S. Cvetkov, "Static Characteristics of the Orifices in a Pilot Operated Pressure Relief Valve", "Hidraulica" (No. 2/2015) Magazine of Hydraulics, Pneumatics, Tribology, Ecology, Sensorics, Mechatronics, ISSN 1453 – 7303, pp.35-39;
- [5] A., Guha, R. M., Barron, R. Balachandar, "An Experimental and Numerical Study of Water Jet Cleaning Process", 2011, "Journal of Materials Processing Technology", pp. 610-618;
- [6] S. J., Leach, G. L. Walker, "Some Aspects of Rock cutting by High Speed Water Jets", July 1966, Philosophical Transactions of the Royal Society of London, Series A, Vol. 260, pp. 295-308;
- [7] M. C. Leu, P. Meng, E. S. Geskin, L. Tismeneskiy, "Mathematical modelling and experimental verification of stationary waterjet cleaning process", August 1998, "Journal of Manufacturing Science and Engineering", Vol. 120, Issue 3, pp.571-579;
- [8] Y. Liu; F. Ma; H. Xie; Y. Li, "Development of Impact Test System for Waterjet Descaling Nozzles with LabVIEW", October 23-24, 2010, International Conference "Web Information Systems and Mining (WISM)", Vol.1, pp.3-7;
- [9] N. Medan, PhD thesis "Research and Contributions to the Functioning of Cleaning Head-Sewer System", November 29, Baia Mare, Romania;
- [10] N. Rajaratnam, C. Albers, "Water Distribution in Very High Velocity Water Jets in Air", June 1998, Vol. 124, No. 6, "Journal of Hydraulic Engineering", ISSN (print): 0733-9429, pp. 647-650.